Theoretical Study of Relationships between Structural, Optical, Energetic, and Magnetic Properties and Reactivity Parameters of Benzidine and Its Oxidized Forms

ARTICLE *in* THE JOURNAL OF PHYSICAL CHEMISTRY A · SEPTEMBER 2014

Impact Factor: 2.69 · DOI: 10.1021/jp507479p · Source: PubMed

2 AUTHORS:

Sergey V Bondarchuk
Cherkasy State University, Bogdan Khmelnitskiy
12 PUBLICATIONS **80** CITATIONS
SEE PROFILE

Boris Minaev
Черкаський національний університ…
328 PUBLICATIONS **3,205** CITATIONS
SEE PROFILE

THE JOURNAL OF PHYSICAL CHEMISTRY A

Article

pubs.acs.org/JPCA

Theoretical Study of Relationships between Structural, Optical, Energetic, and Magnetic Properties and Reactivity Parameters of Benzidine and Its Oxidized Forms

Sergey V. Bondarchuk*[,†] and Boris F. Minaev[†,‡,§]

[†]Department of Organic Chemistry, Bogdan Khmelnitsky Cherkasy National University, blvd. Shevchenko 81, 18031 Cherkasy, Ukraine

[‡]Department of Physics, Tomsk State University, pr. Lenina 36, 634050 Tomsk, Russian Federation

[§]Department of Theoretical Chemistry and Biochemistry, Royal Institute of Technology, AlbaNova, S-106 91 Stockholm, Sweden

Supporting Information

ABSTRACT: Structural, topological, optical, energetic, and magnetic properties and reactivity parameters of benzidine, its radical cation, and its dication as well as molecular complexes of the benzidine dication with the F^-, Cl^-, Br^-, I^-, NO_3^-, HSO_4^-, and $H_2PO_4^-$ anions were calculated at the B3LYP/6-311++G(2d,2p) level of theory in the CH_2Cl_2 medium. The CAM-B3LYP functional (as the most reliable one) and the 6-311++G(3df,3pd) basis set were used for the UV−vis absorption spectra prediction. The obtained spectral results are in a good agreement with available experimental data. A number of the calculated global and local molecular properties, including several recently developed ones, (in general, more than 20 parameters), namely, λ_{max}, the bond lengths and orders (l and $L_{A,B}$), adiabatic ionization energy (IE_{ad}), global electrophilicity index (ω), condensed electrophilic Fukui functions (f^+) and dual descriptor (Δf_A), van der Waals molecular volume, nuclear independent chemical shifts (NICS) and QTAIM topological parameters were estimated in the critical points of the C(1)−C(1′), C(2)−C(3), and C(4)−N bonds as well as at the ring critical point. These quantities were found to be in a strong linear dependence ($R^2 > 0.99$ in most cases) with the number of detached electrons (N_{el}) from the benzidine molecule up to formation of the dication ($N_{el} = 2$). On one hand, a position of the long-wave absorption band (λ_{CT}) corresponding to the anion-to-cation charge transfer in the neutral complexes of the benzidine dication with anions, correlates with the Mulliken electronegativity of the anion ($R^2 = 0.8646$) and its adiabatic ionization energy ($R^2 = 0.8054$). On the other hand, the correlations with the anion charge in the complexes and the anion isotropic polarizability are rather poor ($R^2 = 0.6392$ and 0.3470, respectively). On the ground of the obtained strong relationships, one may recommend the calculated molecular properties as potentially preferable descriptors for the benzidine-based compounds in terms of the QSAR methodology.

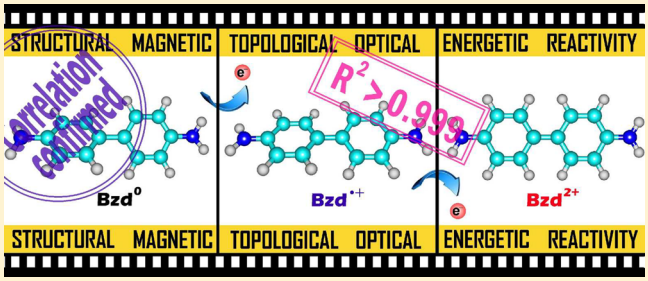

1. INTRODUCTION

Since discovery of its carcinogenicity in far 1970s, benzidine (**Bzd⁰**) became an "outcast" among the potential research objects for more than 30 years. But starting from the mid 2000s, the structural and optical properties of benzidine-based compounds (BBCs) and their oxidized forms, demonstrate a sustainable rising interest of researchers, in particular due to several practical applications.[1−7] Despite the fact that the synthesis of **Bzd⁰** was first reported by Zinin in 1845,[8] an ambiguous structural nature of this compound was clarified not earlier than in 2006 by Rafilovich and Bernstein.[9] They found that **Bzd⁰** exists in four crystal forms corresponding to the $P2_1/n$ (brown-red), $\overline{P}$ (brown-orange), $P2_1/c$ (orange-yellow), and $P2_1/n$ (brown-red) space groups.

Additionally, a considerable attention has been paid to the structural properties of the oxidized forms of **Bzd⁰**,[7,10−18] as well as of the benzidinium salts with inorganic anions.[19−21] In particular, the salts that contain radical cations of benzidine (**Bzd•+**), 3,3′,5,5′-tetramethylbenzidine, 2,2′,6,6′-tetraisopropylbenzidine, and 4,4′-terphenyldiamine with weakly coordinating anions, like $[Al(OC(CF_3)_3)_4]^-$ or SbF_6^-, have been isolated and their UV−vis, ESR, and X-ray spectral data have been recorded.[10] Apart from the structural results, there is a huge body of literature, which relates to some extend with the optical (IR, UV−vis) properties of BBCs; we present a reference list, which does not intend to be fully comprehensive.[1,2,6,22−34]

It is well-known that electrochemical oxidation of BBCs or mixing them with strong oxidants leads to appearance of the color due to formation of the benzidine-based dications (**Bzd²⁺** for benzidine).[25,35] The **Bzd²⁺** dication has a planar quinoid-like

Received: July 25, 2014
Revised: September 3, 2014
Published: September 4, 2014

   dx.doi.org/10.1021/jp507479p | J. Phys. Chem. A 2014, 118, 8872−8882

structure and absorbs always in the visible region. Recently, we have studied theoretically the absorption spectra of BBCs in neutral, radical cation and dication states using CAM-B3LYP/6-311+G(d, p) calculations in the CH_2Cl_2 medium.[7] This functional has been justified as the most reliable one taking into account a careful statistical treatment of the calculated and the known experimental data. It was found that our structural and spectral theoretical results are in a good agreement with the previous experimental studies.[9,10] To the best of our knowledge, there are no data in the literature containing a complete assignment of the **Bzd**^{0}, **Bzd**$^{\bullet+}$, and **Bzd**$^{2+}$ absorption spectra, excluding our recent paper on the latter dication.[7]

The aim of our previous study[7] was to predict position of the λ_{max} for **Bzd**^{0}, its radical cation (**Bzd**$^{\bullet+}$), and dication (**Bzd**$^{2+}$) as well as for several benzidine derivatives in order to use them in a recently developed analytical colorimetric determination of strong oxidants, like the ClO^-, IO_3^-, and BrO_3^- anions, etc.[6] For example, this reaction can be used as an important analytical tool for express testing of the free chlorine content in wastewater or industrial circulating water due to its cheap and easy application. On the other hand, this analytical method can be applied for the BrO_3^- anion determination in such food additives as E924a and E924b being potassium and calcium bromates, respectively. The developed protocol is based on anilines oxidation proceeding via an intermediate formation of BBCs due to anilines oxidative coupling reaction (Scheme 1). The subsequent oxidation of neutral BBCs leads to the colored BBCs dications. Note that the aforementioned stepwise reaction can be altered by a direct BBCs oxidation, but this is less preferable method because of safety reasons. It is worthwhile noting that the most plausible resonance structure of the **Bzd**$^{2+}$ dication is that illustrated in Scheme 1; this follows from our recent QTAIM topological analysis.[36]

An unusual way leading to the **Bzd**$^{2+}$ dication includes self-recombination of the triplet state *p*-$H_2NC_6H_4^+$ cations.[36] These reactive species exhibit an effective positive charge delocalization and a much lower global electrophilicity;[37,38] this allows an effective recombination despite the cationic nature of the reactive species. In contrast to convenient closed-shell carbocations, which have a rather large singlet−triplet gap (*e.g.*, the *p*-methoxybenzhydryl cation has the B3LYP/6-31+G(d,p) estimated gap value to be equal to 38.8 kcal mol^{-1}),[39] the same value for the **Bzd**$^{2+}$ dication is calculated to be only 16.3 kcal mol^{-1} (at the B3LYP/6-311++G(2d,2p) level of theory). Thus, the triplet state of the latter species can be achievable under the dark conditions and should affect the dication reactivity.[40−43]

To prevent the **Bzd**$^{2+}$ dication degradation, the oxidation of BBCs is usually conducted in the acidic media.[6] Thus, the anions, which are present in some excess in the reaction mixture will participate in complexation with the latter dication. This should affect the absorption spectrum of the "pure" **Bzd**$^{2+}$ by appearance of the red-shifted charge transfer bands;[44,45] therefore, one should take into account the possible ion pairing.

Scheme 1. Oxidative Coupling of Anilines Leading to the BBCs Dicationic States

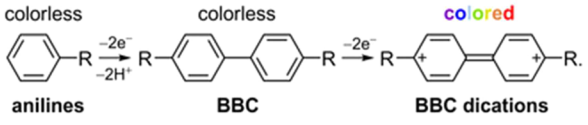

In the previous study we have proposed a model involving the two explicit Cl^- anions being located perpendicular to the **Bzd**$^{2+}$ dication plane (symmetry C_{2h}). This looks like a percent sign, "%" (see Figure 2, below).[7] The model has been successful to describe the spectral behavior of such systems.

The aim of our present work is to study the influence of different counterions, namely the F^-, Cl^-, Br^-, I^-, NO_3^-, HSO_4^-, and $H_2PO_4^-$ anions on the spectral performance of the **Bzd**$^{2+}$ dication. To achieve this goal we used a highly accurate functional determined earlier and an extended basis set (see the following section). In parallel, we have performed a careful analysis of the static global and local properties (structural, topological, optical, energetic, and magnetic ones) as well as some reactivity parameters of the **Bzd**^{0}, **Bzd**$^{\bullet+}$, and **Bzd**$^{2+}$ species. It was found that there is a strong linear correlation between these values corresponding to the neutral, singly and doubly oxidized forms of benzidine. Obviously, the same correlation should be peculiar for various benzidine derivatives; thus, we propose to use the found quantities as the potential quantitative structure−activity relationship (QSAR) descriptors in the study of toxicity of benzidine-based compounds.

2. COMPUTATIONAL DETAILS

Geometry optimization of all studied species has been performed using the density functional theory DFT[46]/B3LYP[47,48] method. Except the iodine atom, the Pople's split-valence triple-ζ basis set (6-311 G) with addition of both polarization (2d, 2p) and diffuse (++) functions[49] was applied during the calculations. The iodine atoms were treated with a pseudopotential, namely, the LANL2DZ basis set.[50] To justify the obtained geometries as the minima, the vibrational frequency analysis was subsequently performed. All the structures considered were characterized by the absence of the imaginary frequencies. Polar medium simulations were done using the polarizable continuum model (PCM).[51] Dichloromethane was chosen as a model solvent because it is the most frequently used one for experimental studies. To define cavities the universal force field (UFF) radii were used.[51] The overlap index and a minimum radius of the spheres were specified as 0.8 and 0.5 Å, respectively.

Electronic spectra were calculated in terms of time-dependent density functional theory (TD DFT). A range-separated hybrid B3LYP functional, which is based on the Coulomb-attenuating method (CAM), namely, CAM-B3LYP,[52] was chosen for the UV−vis spectra prediction because it provides the best fit of the calculated spectra with the known experimental data on BBC's absorption spectra.[7,10] This part of the calculations was performed using a much more extended basis set, namely, the 6-311++G(3df,3pd), except the iodine atoms. These were still treated using the LANL2DZ pseudopotential.

The DFT calculations of the closed-shell species were performed using the spin-restricted Kohn−Sham formalism, while the open-shell species were calculated in terms of the spin-unrestricted Kohn−Sham approach. All the SCF procedures as well as TD DFT calculations were done with the Gaussian09 suite of programs.[53] Fitting the electronic absorption spectra curves were performed using the Gauss distribution function and a half-width of 3000 cm^{-1} with the SWizard 5.0 program package.[54] The quantum theory of atoms in molecules (QTAIM) properties were calculated by the AIMQB program within the AIMStudio suite using the Proaim basin integration method.[55] All post-SCF analyses were

dx.doi.org/10.1021/jp507479p | J. Phys. Chem. A 2014, 118, 8872−8882

conducted using a recently developed Multiwfn program package.[56] Computation of the condensed Fukui functions and the dual descriptor was carried out using the atomic charges determined by the Hirshfeld population analysis.[57] This part of calculations was treated using the DFT(BLYP)/TNP method implemented in Materials Studio 5.5 suite of programs.[58] Wherein, the polar medium simulation was performed using a conductor-like screening model (COSMO).[59]

Among the local molecular properties which were included in the regression analysis we have chosen the electron localization function (ELF),[60] the ELF value determines how the electron motion is confined to a defined molecular spatial region. Another molecular property is the localized orbital locator (LOL).[61] We also estimated local ionization energy ($\overline{I}$) as an essential topological characteristics of a given molecular site.[62] The lower the $\overline{I}(\mathbf{r})$ value, the weaker the electrons are bound at the point with coordinates $\mathbf{r}$.[62] Very important local molecular property is the information (or Shannon) entropy (S). Being introduced in 1948, this quantity was recently found to be a useful tool in theoretical chemistry.[63] An important property for revealing a weak interaction region inside a molecule is sign(λ_2)ρ.[64] This means the sign of the second largest eigenvalue of the electron density Hessian matrix, λ_2, multiplied by the electron density.

A commonly used AIM property, namely, Laplacian of the electron density ($\nabla^2\rho$), was also considered in this work. If $\nabla^2\rho(\mathbf{r}) < 0$, than the electron density is concentrated at the point $\mathbf{r}$. Otherwise, if $\nabla^2\rho(\mathbf{r}) > 0$, then the electron density is depleted from the given molecular site ($\mathbf{r}$).[65] Very informative local AIM functions are the Hamiltonian $h_e(\mathbf{r})$ (or another definition, namely, $K(\mathbf{r})$) and Lagrangian $g(\mathbf{r})$ kinetic energy densities as well as potential energy density $v(\mathbf{r})$.[65] For the bond critical point (3, −1), these can be expressed in terms of the Abramov gradient decomposition.[66−68] Recently, the $g(\mathbf{r})$ values were proposed as a measure for estimating the ring strain energy in cyclic molecules.[69] Another widely used AIM characteristics is an ellipticity of the electron density (ε).[65] This includes λ_1 and λ_2, which are the smallest and the second smallest eigenvalues of the electron density Hessian matrix. These are always negative when estimating at the bond critical point (**BCP**) and demonstrate the curvature of electron density perpendicular to the bond.

The global molecular properties included adiabatic ionization energies (IE_{ad}), which were calculated using eq 1:[36,37,39]

$$\mathrm{IE_{ad}} = U'_0 - U_0 = (E'_{elec} + \mathrm{ZPVE}') - (E_{elec} + \mathrm{ZPVE}) \quad (1)$$

where U_0 and U'_0 are the total energies of a given molecule and its singly oxidized form at 0 K. These are the sums of the corresponding energies at stationary points on the Born−Oppenheimer potential energy surface (E_{elec}) and zero-point vibrational correction (ZPVE).

Global electrophilicity index (ω) was calculated in terms of the Parr scheme (eq 2):[69]

$$\omega = \frac{\mu^2}{2\eta} \quad (2)$$

Herein, $\mu = -(\mathrm{IE_{ad}} + \mathrm{AE_{ad}})/2$ μ and $\eta = \mathrm{IE}_{ad} - \mathrm{EA}_{ad}$, where $\mathrm{IE_{ad}}$ is estimated according to eq 1, while EA_{ad} is an electron affinity, which is calculated in the similar manner (eq 3):[36,37,39]

$$\mathrm{EA_{ad}} = U_0 - U''_0 = (E_{elec} + \mathrm{ZPVE}) - (E''_{elec} + \mathrm{ZPVE}'') \quad (3)$$

where, U''_0 is the total energy of the singly reduced form of a given molecule at 0 K.

The other reactivity parameters are electrophilic Fukui function (f_A^+)[70] and the dual descriptor (Δf_A)[71] condensed to the atom A. An interesting geometry-based quantity aimed to measure aromaticity is the Bird index (I).[72] The most aromatic system should have the Bird index being close to 100.[72] We also calculated the absolute overlap between two orbitals (S_{ij}). We have calculated the overlap integral between the orbitals with numbers 48 and 49. These correspond to the highest occupied (HOMO) and the lowest unoccupied (LUMO) molecular orbitals in the $\mathbf{Bzd^{2+}}$ dication. Thus, when reducing the latter species into the $\mathbf{Bzd^{\bullet+}}$ and, finally, the $\mathbf{Bzd^0}$ molecule, electrons will occupy the MO number 49 and this should increase the overlapping integral. A recently proposed useful molecular property is the Laplacian bond order ($L_{A,B}$).[73] For atoms A and B this can be simply written as

$$L_{A,B} = -10 \times \int_{\nabla^2\rho<0} w_A(\mathbf{r}) w_B(\mathbf{r}) \nabla^2\rho(\mathbf{r})\, d\mathbf{r} \quad (4)$$

where w is a smoothly varying weighting function proposed by Becke and represents fuzzy atomic space.[73]

Finally, we should stress that the molecular van der Waals volume (V_{mol}) was evaluated as the space enclosed by 0.001 isosurface of the electron density using the Monte Carlo method. For more details on the expressions of the rest molecular properties, see the Supporting Information.

3. RESULTS AND DISCUSSION

3.1. Structural Peculiarities of the Benzidine Molecule, Its Oxidized Forms, and Neutral Complexes of the Benzidine Dication with Anions. The optimized structures of benzidine ($\mathbf{Bzd^0}$), its radical cation ($\mathbf{Bzd^{\bullet+}}$) and dication ($\mathbf{Bzd^{2+}}$) are illustrated in Figure 1. Generally, the calculated structural results are in a good agreement with the experimental data on the $\mathbf{Bzd^0}$ ($l_{C(1)-C(1)'}$ = 1.479 Å, $l_{C(2)-C(3)}$ = 1.388 Å, and $l_{C(4)-N}$ = 1.404 Å)[9] and $\mathbf{Bzd^{\bullet+}}$ ($l_{C(1)-C(1)'}$ = 1.432 Å, $l_{C(2)-C(3)}$ = 1.363 Å, and $l_{C(4)-N}$ = 1.342 Å)[10] species. Unfortunately, the $\mathbf{Bzd^{2+}}$ dication is still known only in acidic solutions. This is

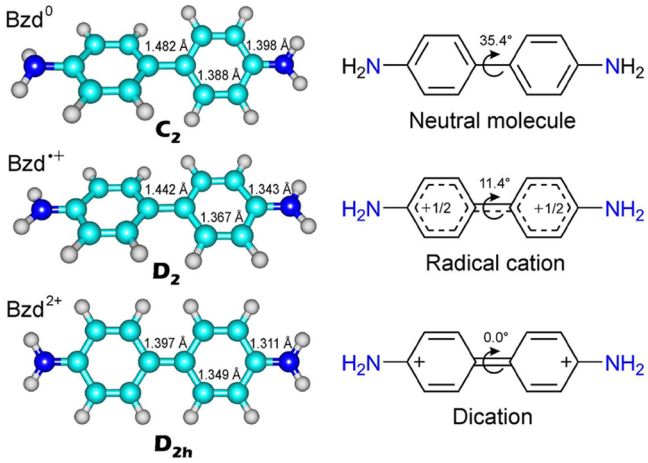

Figure 1. Structure of benzidine ($\mathbf{Bzd^0}$), its radical cation ($\mathbf{Bzd^{\bullet+}}$), and dication ($\mathbf{Bzd^{2+}}$) optimized by the B3LYP/6-311++G(2d,2p) method in the CH_2Cl_2 medium.

dx.doi.org/10.1021/jp507479p | J. Phys. Chem. A 2014, 118, 8872−8882

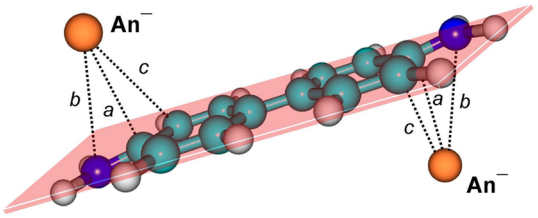

Figure 2. General structure of the neutral complexes $\mathbf{Bzd}^{2+}$ $\mathbf{2An}^{-}$ optimized with the B3LYP/6-311++G(2d,2p) method in the CH_2Cl_2 medium (for iodine the LANL2DZ basis set was used). Herein, An^{-} are the counterions such as the Cl^{-}, Br^{-}, I^{-}, NO_3^{-}, HSO_4^{-}, and $H_2PO_4^{-}$ anions.

Table 1. Structural Parameters *a*, *b*, and *c* (in Å) for the $\mathbf{Bzd}^{2+}$ $\mathbf{2An}^{-}$ Complexes Optimized in This Work[a]

	An^{-}					
	Cl^{-}	Br^{-}	I^{-}	NO_3^{-}	HSO_4^{-}	$H_2PO_4^{-}$
a	3.144	3.325	3.435	2.786	2.967	2.838
b	3.479	3.646	3.831	3.130	3.207	3.124
c	3.471	3.637	3.704	3.135	3.322	3.215

[a]The data are obtained by means of the B3LYP/6-311++G(2d,2p) calculations in the CH_2Cl_2 medium.

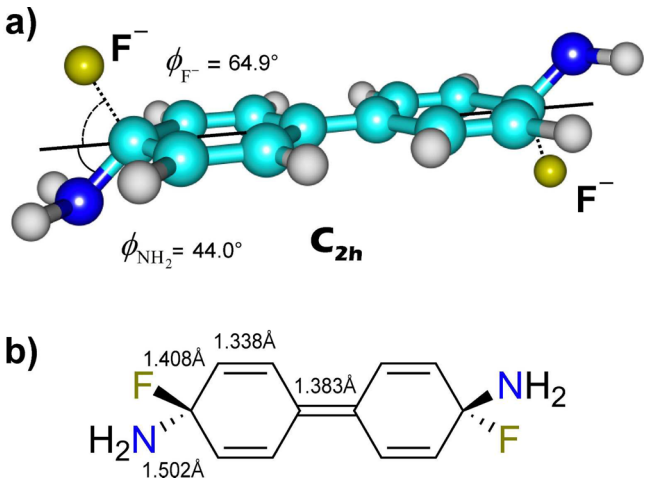

Figure 3. Structure of the neutral covalently bonded complex of the $\mathbf{Bzd}^{2+}$ dication with the fluoride anions optimized with the B3LYP/6-311++G(2d,2p) method in the CH_2Cl_2 medium (top) and the most plausible resonance structure and several bond lengths (bottom).

Table 2. Calculated Values of the Electron Density $\rho(\mathbf{r})$ and Its Laplacian $\nabla^2\rho(\mathbf{r})$ at the BCP between the C(4) or C(4)′ Atoms in the $\mathbf{Bzd}^{2+}$ Dication and the Anion

	An^{-}					
	Cl^{-}	Br^{-}	I^{-}	NO_3^{-}	HSO_4^{-}	$H_2PO_4^{-}$
$\rho(\mathbf{r})$	0.011	0.010	0.017	0.013	0.009	0.011
$\nabla^2\rho(\mathbf{r})$	0.032	0.026	0.029	0.043	0.032	0.038

rather unstable when adjusting the pH higher than 4 and lose color fast.[6] As one can see in Figure 1, the oxidation of the $\mathbf{Bzd}^{0}$ molecule results in a gradual planarization of the benzene nuclei and decreasing the interring torsion angle ($\phi_{int.ring}$); it changes from 35.4° ($\mathbf{Bzd}^{0}$) to 11.4° ($\mathbf{Bzd}^{\bullet+}$) and, finally, to 0.0° in $\mathbf{Bzd}^{2+}$. Such planarization results in a stronger overlap between the rings and formation of a uniform π-conjugated system (D_{2h} symmetry in $\mathbf{Bzd}^{2+}$), a chromophore (Figure 1). Thus, the system changes from a strictly aromatic to a quinoid-like structure. Actually, we not compared the calculated $\phi_{int.ring}$ values and the experimentally determined ones for the $\mathbf{Bzd}^{0}$ and $\mathbf{Bzd}^{\bullet+}$ species because of the known fact about discrepancy between the $\phi_{int.ring}$ values in isolated molecule and a crystal of biphenyl.[74−76] The $\mathbf{Bzd}^{0}$, $\mathbf{Bzd}^{\bullet+}$ and $\mathbf{Bzd}^{2+}$ species are illustrated in their most probable canonical structures (Figure 1, right). Except the $\phi_{int.ring}$ value, the bond lengths $l_{C(1)-C(1)'}$, $l_{C(2)-C(3)}$, and $l_{C(4)-N}$ also suggest the aforementioned conclusion (Figure 1, left). Note that our present structural results on $\mathbf{Bzd}^{0}$ and $\mathbf{Bzd}^{\bullet+}$ are in a good agreement with the experimental data.[9,10]

In our previous topological analysis of the electron density distribution by means of the QTAIM method we have found that the positive charges in $\mathbf{Bzd}^{2+}$ are localized predominantly on the C(4) and C(4)′ atoms.[36] In the radical cation $\mathbf{Bzd}^{\bullet+}$ the charge distribution keeps unchanged, but the values at the C(4) and C(4)′ atoms become close to +1/2 (Figure 1). Single-electron oxidation appears to be not enough to break the aromatic system, which formally remains to be benzenoid. At the same time, the C(4)−N chemical bond and the symmetry equivalent bond possess a partially multiple character (the bond order is about 1.5), which follows from the bond order matrix analysis.

Such gradual transformation from the benzenoid structure to the quinoid-like structure, which accompanies the two-electron oxidation of $\mathbf{Bzd}^{0}$, can be applied for identification of its oxidation state in complex biological systems with cellular macromolecules; hence it may be a criterion for assessing the ability of the benzidine derivative structure to serve as a potential carcinogen. Apart from the structural characteristics, it seems to be possible to use the spectral (optical) structure−activity descriptors, since the aforementioned structural transformations will be accompanied by a bathochromic shift of λ_{max}.

Moreover, we have calculated the neutral complexes of the $\mathbf{Bzd}^{2+}$ dication with some inorganic anions, namely, the F^{-}, Cl^{-}, Br^{-}, I^{-}, NO_3^{-}, HSO_4^{-}, and $H_2PO_4^{-}$ ions. Generally, these monovalent ions coordinate with the $\mathbf{Bzd}^{2+}$ dication plane to form the structures of the C_{2h} symmetry (Figure 2). The optimized structures of the neutral complexes of the $\mathbf{Bzd}^{2+}$ dication with the studied monovalent anions, except F^{-}, namely, the $\mathbf{Bzd}^{2+}$ $\mathbf{2An}^{-}$, are presented in Figure S1 in the Supporting Information. It should be stressed that the discussed structures correspond to the ionically bound (salt-like) molecules. This is supported by the charge distribution in the separated molecular fragments; the anion charges in the complexes are close to −1 (these data will be discussed in more details below). Additionally, the anions coordination corresponds to purely ionic distances (ca. 3.0−4.0 Å). This can be achievable when using a polar medium simulation. In vacuum, the obtained optimized structures appeared to be covalently bound. Once such structures are formed, the sp^2-to-sp^3 rehybridization of the C(4) and C(4)′ atoms occurred.

Another peculiarity of the $\mathbf{Bzd}^{2+}$ $\mathbf{2An}^{-}$ complexes is the anion coordination site. This corresponds to the most positively polarized carbon atoms (C(4) and C(4)′), not the nitrogen atoms. We have denoted the closest contacts between the anion and the organic moiety as the parameters *a*, *b*, and *c* (Figures 2 and S1 in the Supporting Information). The calculated data are listed in Table 1. In the case of the NO_3^{-}, HSO_4^{-}, and $H_2PO_4^{-}$ anions the coordination occurs through the oxygen atom (Figure S1 in the Supporting Information).

dx.doi.org/10.1021/jp507479p | J. Phys. Chem. A 2014, 118, 8872−8882

Table 3. Assignment of the Absorption Bands in the Electronic Spectrum of the Bzd^{2+} Dication Calculated at the CAM-B3LYP/6-311++G(3df,3pd) Level of Theory in the CH_2Cl_2 Medium (f = Oscillator Strength)

state	λ, nm	f	assignment	symmetry
S_1	**429**	**1.4683**	**HOMO → LUMO (100%)**	**B_{1u}**
S_{13}	189	0.3496	HOMO − 2 → LUMO + 1 (85%)	B_{2u}
S_{15}	180	0.5777	HOMO − 1 → LUMO + 2 (51%)	B_{1u}
			HOMO → LUMO + 7 (27%)	
S_{17}	175	0.5894	HOMO → LUMO + 7 (45%)	B_{1u}
			HOMO − 1 → LUMO + 2 (27%)	B_{1u}
			HOMO − 3 → LUMO + 1 (22%)	B_{1u}

Table 4. Assignment of the Absorption Bands in Electronic Spectrum of the $Bzd^{\bullet+}$ Radical Cation Calculated Using the DFT(CAM-B3LYP)/6-311++G(3df,3pd) Method in the CH_2Cl_2 Medium

state	λ, nm	f	assignment	symmetry
S_1	780	0.5260	HOMO(β) → LUMO(β) (96%)	B_1
S_4	**378**	**0.5643**	**HOMO(α) → LUMO(α) (83%)**	**B_3**
S_9	280	0.0662	HOMO − 2(α) → LUMO + 1(α) (24%)	B_3
			HOMO − 1(β) → LUMO + 2(β) (19%)	B_3
			HOMO − 3(α) → LUMO + 3(α) (16%)	A
			HOMO − 2(β) → LUMO + 6(β) (11%)	B_3
S_{13}	238	0.1059	HOMO − 5(β) → LUMO(β) (72%)	B_1
S_{33}	190	0.4862	HOMO − 1(β) → LUMO + 2(β) (28%)	B_3
			HOMO − 2(α) → LUMO + 1(α) (18%)	B_3
			HOMO − 10(β) → LUMO(β) (18%)	B_3
S_{35}	190	0.3706	HOMO − 2(β) → LUMO + 1(β) (61%)	A
			HOMO − 3(α) → LUMO(α) (20%)	A

Table 5. Assignment of the Absorption Bands in Electronic Spectrum of Neutral Benzidine Calculated at the CAM-B3LYP/6-311++G(3df,3pd) Level of Theory in the CH_2Cl_2 Medium

state	λ, nm	f	assignment	symmetry
S_2	**274**	**0.8702**	**HOMO → LUMO + 1 (89%)**	**B**
S_3	269	0.0643	HOMO → LUMO + 5 (64%)	A
S_{10}	207	0.0802	HOMO → LUMO + 8 (49%)	B
S_{13}	204	0.1525	HOMO → LUMO + 10 (74%)	B
S_{18}	195	0.3902	HOMO − 3 → LUMO + 1 (55%)	A
S_{19}	194	0.8931	HOMO − 2 → LUMO + 3 (53%)	A
			HOMO − 3 → LUMO + 5 (30%)	B

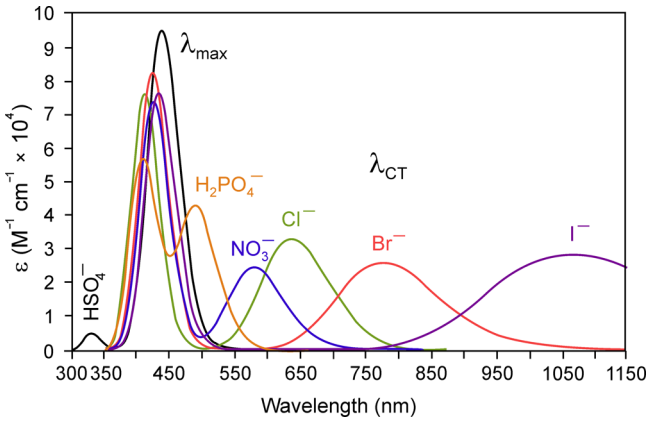

Figure 4. UV−vis absorption spectra of the neutral complexes **Bzd^{2+} $2An^-$** calculated with the B3LYP/6-311++G(3df,3pd) method in the CH_2Cl_2 medium. Herein, An^- are the Cl^-, Br^-, I^-, NO_3^-, HSO_4^-, and $H_2PO_4^-$ anions.

The nitrate anion triangles lie at the perpendicular orientation to the **Bzd^{2+}** dication plane, while the both hydrogen sulfate and dihydrogen phosphate ions are arranged in such way that the hydroxo groups are turned out of the dications plane (Figure S1 in the Supporting Information).

Table 6. Position of the Shortwave Absorption Band (λ_{max}) and the Longwave Absorption Band (λ_{CT}) for the Bzd^{2+} $2An^-$ Complexes Studied in This Work, Except the Fluoride Anions[a]

	An^-					
	Cl^-	Br^-	I^-	NO_3^-	HSO_4^-	$H_2PO_4^-$
λ_{max}	409	421	432	423	436	410
λ_{CT}	637	776	1048	578	333	489

[a]The spectral wavelengths are obtained using the CAM-B3LYP/6-311++G(3df,3pd) calculations in the CH_2Cl_2 medium and presented in nm.

On the other hand, the optimized structure of the **Bzd^{2+} $2F^-$** complex exhibits a different geometry (Figure 3). Despite the PCM simulation applied, the **Bzd^{2+} $2F^-$** complex is covalently rather than ionically bound. The C(4) and C(4)′ atoms are sp^3 hybridized; therefore, the fluorine atoms and amino groups lie out of the rings plane and form dihedral angles with the latter ϕ_{F^-} and ϕ_{NH_2}, respectively (Figure 3). The atomic charges at

dx.doi.org/10.1021/jp507479p | J. Phys. Chem. A 2014, 118, 8872−8882

Table 7. Correlation between the λ_{CT} Values and Several Parameters of the Anions[a]

entry	Cl^-	Br^-	I^-	NO_3^-	HSO_4^-	$H_2PO_4^-$	R^2
χ	2.35	2.54	1.36	3.01	3.20	3.26	0.8646
IE_{ad}	6.37	6.04	5.94	6.23	6.77	6.31	0.8054
q_{An}	−0.948	−0.862	−0.607	−0.839	−0.908	−0.879	0.6392
α	29.84	44.34	83.39	36.07	49.09	52.87	0.3470

[a]Herein, χ is the Mulliken electronegativity (in eV), IE_{ad} is the adiabatic ionization energy (in eV), q_{An} is the anion total charge in the $\mathbf{Bzd^{2+}}$ $\mathbf{2An^-}$ complexes, and α is isotropic polarizability (in $bohr^3$).

the fluorine atoms are equal to −0.571 and the nitrogen atoms are pyramidalized suggesting the zero-charged benzidine framework. The C−F bond length is equal to 1.408 Å similar to that of CH_3F (1.39 Å).[77]

The final verdict about the nature of the C−F bond in the $\mathbf{Bzd^{2+}}$ $\mathbf{2F^-}$ complex can be obtained in terms of the QTAIM electron density analysis. It is known that a good criterion of the bond types are the values of electron density $\rho(\mathbf{r})$ and its Laplacian $\nabla^2\rho(\mathbf{r})$ at the **BCP**.[65] If $\rho(\mathbf{r})$ is close to 0.1 and $\nabla^2\rho(\mathbf{r}) \ll 0$, than the given bond is *shared* (covalent or polar).[65] In contrast, if $\rho(\mathbf{r})$ is about 0.01 and $\nabla^2\rho(\mathbf{r}) > 0$, than the considered bond corresponds to a closed-shell interaction (the *ionic* bond).[65] However, we should stress that there are other classifications of chemical bonds, in particular, on the ground of the $\nabla^2\rho(\mathbf{r})$ and $h_e(\mathbf{r})$ values.[78,79] At the C−F bond critical point in the $\mathbf{Bzd^{2+}}$ $\mathbf{2F^-}$ complex the calculated $\rho(\mathbf{r})$ value is equal to 0.19, while $\nabla^2\rho(\mathbf{r}) = -0.218$. Thus, one can conclude that this bond has the covalent nature. The $\rho(\mathbf{r})$ and $\nabla^2\rho(\mathbf{r})$ values in the bond critical point between the anion and cation are listed in Table 2 for the rest studied complexes.

As one can see in Table 2, all the rest of the cation−anion interactions should be interpreted as typically ionic.[65] We should stress that in the case of the $\mathbf{Bzd^{2+}}$ $\mathbf{2Cl^-}$, $\mathbf{Bzd^{2+}}$ $\mathbf{2Br^-}$, $\mathbf{Bzd^{2+}}$ $\mathbf{2I^-}$, and $\mathbf{Bzd^{2+}}$ $\mathbf{2HSO_4^-}$ complexes the **BCP** between the cation and anion is formed only with the C(4) as well as the C_{2h}-symmetric carbon atom. In contrast, the complexation of the NO_3^- and $H_2PO_4^-$ anions occur simultaneously through the other ring carbon atoms and the anion oxygen atoms (see Figure S1 in the Supporting Information for clarity), but the aforementioned QTAIM properties in these **BCPs** have the same nature as those discussed in Table 2.

Such unusual structural results on the $\mathbf{Bzd^{2+}}$ $\mathbf{2F^-}$ complex suggest the possible calculation artifact. Indeed, the latter could arise from a lack of long-range correction in the functional used (the B3LYP) and from improper starting geometry guess. In order to explore these two possible reasons, we have calculated the fluorine complex using five various long-range functionals, namely, CAM-B3LYP, wB97xD, LC-wPBE, wB97X, and LC-BLYP. As the starting geometry guess we have chosen the stationary geometry of the corresponding chlorine complex. Thus, the C(4)−F interatomic distances were equal to 3.14 Å—more than enough to fall into a minimum corresponding to the ionic bonding type complex. As expected, all these calculations have led to the same covalently bound complex, like with the use of the B3LYP functional that follows from the C(4)−F interatomic distance values (Table S1 in the Supporting Information).

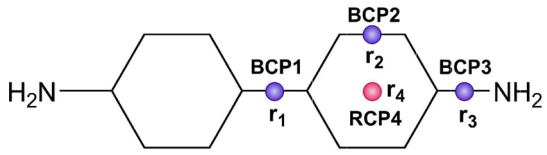

Figure 5. Bond (**BCP**) and ring (**RCP**) critical points in which the local descriptors are estimated.

To be sure that no other minimum is present along the potential energy surface (PES) profile, we have performed the relaxed scan optimization of the latter. We have used the long-range functional, namely, the CAM-B3LYP and the 6-311++G(2d,2p) basis set in CH_2Cl_2 medium. As the starting geometry of the calculation, we have used the covalently bound complex. The step size was specified as 0.25 Å and the scan was proceeded until the C(4)−F interatomic distance became equal to 3.75 Å. The calculations revealed that there is no other minimum along the PES profile. When the fluorine atoms leave the $\mathbf{Bzd^{2+}}$ dication, the energy gradually rises and converges to the dissociation limit (Figure S2 in the Supporting Information). Thus, we believe that there is no calculation artifact in the present results.

3.2. Assignment of Absorption Bands in Electronic Spectrum of Benzidine and its Oxidation Products.

Absorption spectrum of the $\mathbf{Bzd^{2+}}$ dication was recently studied theoretically.[7] It has been shown that λ_{max} corresponds to the HOMO → LUMO transition. These MOs are the purely benzene orbitals and, therefore, the aforementioned electron transition corresponds to a local excitation in the aromatic system without significant charge transfer contribution.[7] Although the $\mathbf{Bzd^{2+}}$ dication has a quinoid-like structure rather than benzenoid (Figure 1), it still remains to be a weakly aromatic species, which follows from the corresponding NICS and Bird aromaticity criteria below.

Because of the D_{2h} symmetry of the $\mathbf{Bzd^{2+}}$ dication there are only four intense bands in the near-middle UV−vis electronic spectrum. Herein, we present spectra calculation results using the DFT(CAM-B3LYP)/6-311++G(3df,3pd) method (Table 3). Meanwhile, the preliminary data regarding to the CAM-B3LYP/6-311+G(d,p) calculation results are presented in Table S2 in the Supporting Information. We should stress that the approach used in this work provides an exact coincidence of the λ_{max} position in the $\mathbf{Bzd^{2+}}$ dication absorption spectrum with the experimental data.[4,80] The results of the $\mathbf{Bzd^{\bullet+}}$ and $\mathbf{Bzd^0}$ electronic spectra calculations are listed in Tables 4 and 5, respectively. In Tables 3−5 all the bands with oscillator strength (f) being lower than 0.05 are omitted for simplicity, while the bands corresponding to λ_{max} are highlighted with boldface.

Table 8. Correlation of the Structural Parameters

N_{el}	$l_{C(1)-C(1')}$	$l_{C(2)-C(3)}$	$l_{C(4)-N}$	$L_{C(1)-C(1')}$	$L_{C(2)-C(3)}$	$L_{C(4)-C(N)}$
0	1.482	1.388	1.398	1.053 701	1.444 344	0.923 393
1	1.442	1.367	1.343	1.207 204	1.545 36	1.117 864
2	1.397	1.349	1.311	1.412 347	1.656 079	1.320 234
R^2	0.9988	0.9980	0.9772	0.9931	0.9993	0.9999

dx.doi.org/10.1021/jp507479p | J. Phys. Chem. A 2014, 118, 8872−8882

Table 9. Correlation of the Global Molecular Properties

N_{el}	λ_{max}	V_{mol}	IE_{ad}	ω	$f^{+}_{(C1)}$ [a]	$\Delta f_{(C1)}$	NICS(1) [b]	I	S_{ij}	$q_{C(4)}$ [c]	$q_{C(1)}$
0	274	252.723	5.00	1.10	0.037	−0.010	−8.4	94.81	0.9086	0.364 17	−0.015 10
1	375	240.798	6.11	13.49	0.047	−0.004	−5.4	78.38	0.8892	0.493 92	0.005 49
2	429	231.004	8.41	11.20	0.054	−0.001	−2.9	60.68	0.8677	0.598 03	0.035 64
R^2	0.9711	0.9968	0.9610	0.5868	0.9897	0.9643	0.9973	0.9995	0.9992	0.9960	0.9883

[a]Radical, electrophilic and nucleophilic Fukui functions condensed to all the symmetry unique atoms are presented in Table S6 in the Supporting Information. [b]The NICS values up to 3 Å are listed in Table S7 in the Supporting Information. [c]The QTAIM charges at all the symmetry unique atoms are presented in Table S8 in the Supporting Information.

Table 10. Correlation of the Local Molecular Properties at the r_2 Point (BCP2)

N_{el}	ELF(r)	LOL(r)	$\overline{I}$(r)	S(r)	Ω(r)	$\nabla^2\rho$(r)	K(r)	v(r)	g(r)	ε(r)
0	0.940 05	0.798 40	0.568 53	0.181 87	−0.309 57	−0.859 33	0.317 54	−0.420 24	0.102 71	0.223 44
1	0.936 88	0.793 93	0.616 83	0.189 36	−0.321 76	−0.921 61	0.343 00	−0.455 59	0.112 60	0.246 47
2	0.933 95	0.789 94	0.669 86	0.196 76	−0.333 61	−0.983 84	0.368 48	−0.491 00	0.122 52	0.268 55
R^2	0.9995	0.9989	0.9993	1.0000	0.9999	1.0000	1.0000	1.0000	1.0000	0.9999

Table 11. Correlation of the Local Molecular Properties at the r_4 Point (RCP4)

N_{el}	ELF(r)	LOL(r)	$\overline{I}$(r)	S(r)	Ω(r)	$\nabla^2\rho$(r)	K(r)	v(r)	g(r)	ε(r)
0	0.218 07	0.129 95	0.688 13	0.184 48	0.214 54	0.157 21	−0.007 46	−0.024 38	0.031 84	−1.203 86
1	0.211 34	0.128 15	0.730 34	0.181 85	0.208 93	0.153 43	−0.007 40	−0.023 56	0.030 96	−1.200 69
2	0.205 21	0.126 48	0.776 64	0.178 06	0.201 88	0.147 75	−0.007 26	−0.022 42	0.029 68	−1.194 97
R^2	0.9993	0.9995	0.9993	0.9892	0.9957	0.9867	0.9494	0.9912	0.9887	0.9733

A characteristic feature of the absorption spectra of **Bzd^0** and **Bzd$^{\bullet+}$** is that they are formally similar to the previously studied spectrum of **Bzd^{2+}**.[7] The λ_{max} value regularly changes during oxidation of **Bzd^0** into **Bzd^{2+}** species. It linearly increases from 274 to 378 and, finally, up to 429 nm (Tables 3−5). In the case of the **Bzd$^{\bullet+}$** radical cation absorption spectrum, λ_{max} corresponds to the HOMO(α) → LUMO(α) transition and is related to a local ring excitation. Though, the λ_{max} value corresponds to the S_4 state, the first S_1 state has very close oscillator strength (Table 4). Indeed, the **Bzd$^{\bullet+}$** radical cation absorption spectrum has two the most intense bands in the visible region which is in accord with the recent experimental and theoretical CAM-B3LYP/6-31+G(d,p) results.[10] The situation when λ_{max} is not the first excited state S_1 is also peculiar for the **Bzd^{2+}** dication UV−vis spectrum in vacuum[7] and also for the neutral **Bzd^0** species (Table 5). Thus, the S_2 state corresponds to λ_{max}, while the S_1 state has f = 0. This reveals that the **Bzd^{2+}** dication absorption spectrum is very solvent-dependent. Taking into account this dication peculiarity one can assume that fluorescence may occur from the higher excited states, like in azulenes and analogues,[81] or can be quenched depending on the solvent.

Most of the absorption bands in the electronic spectra of the **Bzd$^{\bullet+}$** and **Bzd^0** species (Table 4 and 5) correspond to the local excitation in the π system (see also Figures S3 and S4 in the Supporting Information). But some bands have a partial charge transfer contribution from the π system to the amino group (states S_{33} and S_{35} in Table 4 and also S_3 and S_{18} in Table 5). It is important to note that a bathochromic shift of the λ_{max} value caused by oxidation can be rationalized by the formation of a uniform π-conjugated system being a typical chromophore. Moreover, the strong auxochromes, like the NH_2 group, enhance color due to the donation of two p electrons into the π system. These factors provide the BBC dications to have clear colors; this molecular characteristic is now actively used in colorimetric determination of strong oxidants.[6] Thus, it is important to know how the explicit anions, formed after BBC oxidation, affect the absorption spectrum of the isolated dication, especially the λ_{max} value.

3.3. Account of the Influence of Explicit Anions on the Benzidine Dication Electronic Spectrum. The results of the spectra calculations listed in the previous section are performed in terms of a rather crude approximation. This is due to neglect of electrostatic influence of the explicit counterions. This effect can be taken into account using the known QM/MM technique when the organic fragment is treated at quantum level, while the explicit ionic environment at is treated at the molecular mechanical level. Also the effect of counterions can be included by means of the Monte Carlo method or molecular dynamics. On the other hand, in our recent work we have found that a molecular model including two explicit monovalent anions (see section 3.1) provide rather reliable spectral results.[7]

We have calculated the electronic spectra of all the complexes described in section 3.1. Graphically, the results are illustrated in Figure 4. As one can see in Figure 4 the absorption spectra are characterized by the two intense bands. One of them (a shortwave) corresponds to λ_{max} and has the same nature as in the isolated dication (Table 3), while the longwave bands (λ_{CT}) correspond to the anion-to-cation charge transfer. These predominantly consist of several low-intensity bands, whose superposition provides an increased total absorption (Figure 4).

It is interesting that the nature of the anion does not affect markedly the position of λ_{max}, but strongly affects the position of λ_{CT} (Figure 4). The various anions have their own specific λ_{CT} values; thus, the aforementioned colorimetric method can be used for simultaneous qualitative determination of the present anions. The absorption of the **Bzd^{2+} 2HSO$_4^-$** complex has a different spectral picture; its λ_{CT} band lies at 333 nm and has a very low intensity (Figure 4, the black curve). Indeed, when the colorimetric reaction is proceeding in solution of sulfuric acid, the experimental absorption spectrum of the reaction mixture exhibits no absorption beyond the 475 nm (in

dx.doi.org/10.1021/jp507479p | J. Phys. Chem. A 2014, 118, 8872−8882

the case of diethylaniline as the starting amine).[6] On the other hand a small peak is appeared at 325 nm,[6] which can be reliably ascribed to λ_{CT}. Thus, the present molecular model completely confirms the available experimental data. All the calculated values of λ_{max} and λ_{CT} are listed in Table 6.

We have tried to rationalize which factors affect the position of λ_{CT}. Naturally, the molecular properties concerned with ability of the anion to release an electron should be closely related to the position of λ_{CT}. We have analyzed four parameters of the anions, which are listed in Table 7, and compared them with the λ_{CT} position. As one can see in Table 7, the best correlated values are χ and IE_{ad}, while q_{An} and α provide much poorer correlation. Thus, when known the χ value of the anion, it is possible to estimate the relative position of λ_{CT} and, therefore, the final color of the reaction mixture. It is clear that such compounds as orthophosphate, nitric, hydrochloric and, partly, hydrobromic acids will mask the color of "pure" dication.

In the case of the $\mathbf{Bzd^{2+}}$ $\mathbf{2F^-}$ complex, the calculated UV−vis spectral data additionally suggest the covalently bound structure (Figure 3). The absorption spectrum of this compound also includes two intense bands at 345 nm (λ_{max}) and 239 nm (Table S3 in the Supporting Information). For understanding the molecular orbital nature, see Figure S5 in the Supporting Information. Thus, λ_{max} lies in the near UV region and has a different nature than that of the other complexes. For the fluoride anion the aforementioned parameters are the following: α = 7.22 Bohr^3, χ = 0.77 eV, IE_{ad} = 6.78 eV, and q_{An} = −0.571. The values of isotropic polarizability and Mulliken electronegativity much differ from that of the other anions; therefore, we anticipate that a comprehensive study of the different anion (nucleophile) properties in terms of conceptual DFT can provide a valuable insight into the BBC dications reactivity toward nucleophilic addition or substitution.

3.4. Relationships between Topological Parameters of Benzidine, Its Radical Cation and Dication. Relationships between topological parameters of benzidine and its oxidation products are directly related with a known problem of *isoelectronic systems*. If one consider a complex between two separate molecular fragments A and B this problem can be schematically illustrated as the following:

$$[A\cdots B],\ [A^+\cdots B^-],\ [A^{2+}\cdots B^{2-}],\ [A^-\cdots B^+],\ \text{etc.}$$

The different fragments can have different oxidation states; therefore, its identification is complicated. This is a very important issue in studying carcinogenicity of the benzidine family compounds. It is known that benzidine, in the form of monocation (aryl nitrenium ion), binds covalently to cellular macromolecules, especially DNA, forming the *N*-acetylated guanine.[24] Thus, oxidation state of the benzidine fragment in the complexes with macromolecules is very important, especially when the hydrogen bonds are encountered.

Simple DFT calculations, however, are able to solve this problem because the structural and other local and global molecular parameters of benzidine are in a strong linear dependence with the number of detached electrons (the total molecular charge). On the other hand, such strongly correlated quantities can be applied as potentially favorable structure−activity descriptors for both the benzidine family and the related ones. In this study, we have checked a great number of different topological parameters and the most successful ones have been included in this paper and described in the Computational Details.

First of all, we have found that three structural parameters (the bond lengths and their orders) are strongly correlated. These values are listed in Table 8. Note that the atom labeling is illustrated in Figure S6 in the Supporting Information. The global molecular parameters have been calculated regarding to the whole molecule, while the local characteristics have been estimated in **BCPs** of the aforementioned bonds as well as in the ring critical point **RCP** (Figure 5). The calculated data are presented in Tables 9−11. Among the local parameters the best correlation has been found for the values corresponding to **BCP2** (Table 10). At the same time, the analogous values for **BCP1** and **BCP3** are collected in Tables S4 and S5 in the Supporting Information, respectively. We anticipate that all these correlations can be valid for various benzidine or even byphenyl derivatives, in general. Therefore, the QSAR studies of the described molecular parameters are of great interest.

As it follows from Table 9, most of the global molecular properties change linearly during the oxidation. In particular, local electrophilicity rises gradually, which is seen from the $f^+_{(C1)}$, $\Delta f_{(C1)}$ values and QTAIM charges at the C(4) and C(1) atoms. The latter charges as well as the aromaticity parameters, namely, NICS(1) and the Bird index *I* also suggest the formation of the quinoid-like structure of the $\mathbf{Bzd^{2+}}$ dication (Figure 1). A strongly aromatic nature of $\mathbf{Bzd^0}$ changes to a slightly aromatic in the $\mathbf{Bzd^{2+}}$ dication (Table 9).[36] On the other hand, the global electrophilicity index of the dication is lower than that of the radical cation (11.20 versus 13.49 eV). This circumstance is the reason for such a low regression coefficient (R^2 = 0.5868).

The local molecular parameters calculated in the points $\mathbf{r_2}$ and $\mathbf{r_4}$ display an excellent correlation (Tables 10 and 11). Often the R^2 value is equal to 1 or extremely close to.

4. CONCLUSIONS

In this paper, we describe a comprehensive theoretical study of the structure, spectra and topological parameters of benzidine and its oxidation products. On the ground of a complete assignment of the absorption bands in electronic spectra of the latter species by means of a very accurate approach, namely, CAM-B3LYP/6-311++G(3df,3pd) in the CH_2Cl_2 medium, the nature of λ_{max} was ascribed to a local excitation in the benzene nuclei without the charge transfer contribution. The position of λ_{max} strongly correlates with the number of detached electrons and displays a redshift from 274 nm (in $\mathbf{Bzd^0}$) to 378 nm (in $\mathbf{Bzd^{\bullet+}}$) and, finally, to 429 nm (in $\mathbf{Bzd^{2+}}$) during the oxidation. These results are in an excellent agreement with the available experimental data.[1,2,6,22−34] The bathochromic shift is caused by the planarization of the nuclei and the formation of a uniform conjugated π system (a chromophore).

The influence of explicit anions on the "pure" $\mathbf{Bzd^{2+}}$ dication spectrum is studied for the F^-, Cl^-, Br^-, I^-, NO_3^-, HSO_4^-, and $H_2PO_4^-$ ions. The effect of the latter is in appearance of a broad anion-to-cation charge transfer band (λ_{CT}). Except the hydrosulfate anion (333 nm), it is shifted bathochromically to the region of 489−1048 nm depending on the anion. The position of λ_{CT} is well described by the Mulliken electronegativity and adiabatic ionization energy values of the corresponding anion. Again, the developed C_{2h} symmetrical molecular model provides spectral results, which completely conform the known experimental findings.[6] The nature of anion changes sharply the spectrum of the bare dication, which is very important for analysts who work with these compounds.

dx.doi.org/10.1021/jp507479p | J. Phys. Chem. A 2014, 118, 8872−8882

Finally, the topological analysis of the studied species revealed a number of potential descriptors (more than 20) which can be applied in QSAR methodology for identification of the oxidation state of BBCs in the complexes with cellular macromolecules. Excluding the ω values, the screened global molecular properties provide an average regression coefficient being equal to 0.9863. The local parameters at the $\mathbf{r}_4$ point display similar average value (R^2 = 0.9872), while the ones at the $\mathbf{r}_2$ point yield the best average value to be equal to 0.9998.

■ ASSOCIATED CONTENT

Supporting Information

Additional information concerning complete ref 53, structures of the neutral complexes of the benzidine dication with anions, complete assignment of electronic spectra, molecular orbital energy diagrams, radical, electrophilic and nucleophilic Fukui functions, the NICS values, and the QTAIM charges concerning the studied species. This material is available free of charge via the Internet at http://pubs.acs.org.

■ AUTHOR INFORMATION

Corresponding Author

*(S.V.B.) Fax: (+3) 80472 37-21-42. Telephone: (+3) 80472 37-65-76. E-mail: bondchem@cdu.edu.ua.

Notes

The authors declare no competing financial interest.

■ ACKNOWLEDGMENTS

This work was supported by the Ministry of Education and Science of Ukraine, Research Fund (Grant No. 0113U001694). We thank Professor Hans Ågren (KTH, Stockholm) for the PDC supercomputer use. The computations were performed on resources provided by the Swedish National Infrastructure for Computing (SNIC) at the Parallel Computer Center (PDC) through the project "Multiphysics Modeling of Molecular Materials", SNIC 020/11-23.

■ REFERENCES

(1) Yurchenko, O.; Freytag, D.; zur Borg, L.; Zentel, R.; Heinze, J.; Ludwigs, S. Electrochemically Induced Reversible and Irreversible Coupling of Triarylamines. *J. Phys. Chem. B* **2012**, *116*, 30−39.

(2) Matis, M.; Rapta, P.; Lukes, V.; Hartmann, H.; Dunsch, L. Highly Charged Cations from *N,N,N′,N′*-Tetrakis(4-aminophenyl)benzidine and Its *N,N,N′,N′*-Tetrakis(4-methoxyphenyl)-Substituted Homologue Studied by Thin-Layer in Situ Electron Spin Resonance/UV−Vis−NIR Spectroelectrochemistry. *J. Phys. Chem. B* **2010**, *114*, 4451−4460.

(3) Minaev, B. F.; Li, X.; Ning, Zh.; Tian, H.; Ågren, H. Organometallic Materials for Electroluminescent and Photovoltaic Devices. In *Orgnic Light Emiting Diode—Materials, Processes and Devices*; Ko, S. H., Ed.; InTech: Rijeka, Croatia, 2011; Vol. 3, pp 61−100.

(4) Rapta, P.; Zeika, O.; Rohde, D.; Hartmann, H.; Dunsch, L. Thiophene−Thiophene versus Phenyl−Phenyl Coupling in 2-(Diphenylamino)-Thiophenes: An ESR-UV/Vis/NIR Spectroelectrochemical Study. *ChemPhysChem.* **2006**, *7*, 863−870.

(5) Marjanović, B.; Juranić, I.; Ćirić-Marjanović, G. Revised Mechanism of Boyland−Sims Oxidation. *J. Phys. Chem. A* **2011**, *115*, 3536−3550.

(6) Zaporozhets, O. A.; Pogrebnyak, O. S.; Vizir, N. N. Spectrophotometric Determination of Oxyhalides with N,N-Diethylaniline. *J. Anal. Chem.* **2012**, *67*, 694−700.

(7) Bondarchuk, S. V.; Minaev, B. F. Electronic Descriptors for Analytical Use of the Benzidine-Based Compounds and the Mechanism of Oxidative Coupling of Anilines. *J. Phys. Org. Chem.* **2014**, *27*, 640−651.

(8) Zinin, N. Ueber das Azobenzid und die Nitrobenzinsäure. *J. Prakt. Chem.* **1845**, *36*, 93−107.

(9) Rafilovich, M.; Bernstein, J. Serendipity and Four Polymorphic Structures of Benzidine, $C_{12}H_{12}N_2$. *J. Am. Chem. Soc.* **2006**, *128*, 12185−12191.

(10) Chen, X.; Ma, B.; Wang, X.; Yao, S.; Ni, L.; Zhou, Z.; Li, Y.; Huang, W.; Ma, J.; Zuo, J.; Wang, X. From Monomers to π Stacks, from Nonconductive to Conductive: Syntheses, Characterization, and Crystal Structures of Benzidine Radical Cations. *Chem.—Eur. J.* **2012**, *18*, 11828−11836.

(11) Jacob, J. A.; Naumov, S.; Biswas, N.; Mukherjee, T.; Kapoor, S. Comparative Study of Ionization of Benzidine and Its Derivatives by Free Electron Transfer and One-Electron Oxidation. *J. Phys. Chem. C* **2007**, *111*, 18397−18404.

(12) Masson, E. Torsional Barriers of Substituted Biphenyls Calculated Using Density Functional theory: A Benchmarking Study. *Org. Biomol. Chem.* **2013**, *11*, 2859−2871.

(13) Ghigo, G.; Osella, S.; Maranzana, A.; Tonachini, G. The Mechanism of the Acid-Catalyzed Benzidine Rearrangement of Hydrazobenzene: A Theoretical Study. *Eur. J. Org. Chem.* **2011**, 2326−2333.

(14) Yamabe, Sh.; Nakata, H.; Yamazaki, S. π Complexes in Benzidine Rearrangement. *Org. Biomol. Chem.* **2009**, *7*, 4631−4640.

(15) Ghigo, G.; Maranzana, A.; Tonachini, G. A Change from Stepwise to Concerted Mechanism in the Acid-Catalysed Benzidine Rearrangement: A Theoretical Study. *Tetrahedron* **2012**, *68*, 2161−2165.

(16) Sarkar, U.; Roy, D. R.; Chattaraj, P. K.; Parthasarathi, R.; Padmanabhan, J.; Subramanian, V. A Conceptual DFT Approach towards Analysing Toxicity. *J. Chem. Sci.* **2005**, *117*, 599−612.

(17) Chung, K. Th.; Chen, S.-Ch; Wong, T. Y.; Li, Y.-S.; Wei, Ch.-I.; Chou, M. W. Mutagenicity Studies of Benzidine and Its Analogs: Structure-Activity Relationships. *Toxicol. Sci.* **2000**, *56*, 351−356.

(18) Akalin, E.; Akyüz, S. Structure and Vibrational Spectra of Benzidine. *J. Mol. Struct.* **2003**, *651−653*, 571−577.

(19) Smith, G.; Wermuth, U. D.; White, J. M. Mixed Dicationic and Monocationic Benzidine Species in the Proton-Transfer Compound of Benzidine qith 3,5-Dinitrosalicylic Acid. *Acta Crystallogr.* **2006**, *C62*, o402−o404.

(20) Dobrzycki, L.; Woźniak, K. 1D vs 2D Crystal Architecture of Hybrid Inorganic−Organic Structures with Benzidine Dication. *J. Mol. Struct.* **2009**, *921*, 18−33.

(21) Dobrzycki, L.; Woźniak, K. Structures of Hybrid Inorganic−Organic Salts with Benzidine Dication Derivatives. *CrystEngComm.* **2008**, *10*, 525−533.

(22) Hmadeh, M.; Traboulsi, H.; Elhabiri, M.; Braunstein, M.; Albrecht-Gary, A.-M.; Siri, O. Synthesis, Characterization and Photophysical Properties of Benzidine-Based Compounds. *Tetrahedron* **2008**, *64*, 6522−6529.

(23) Kirchgessner, M.; Sreenath, K.; Gopidas, K. R. Understanding Reactivity Patterns of the Dialkylaniline Radical Cation. *J. Org. Chem.* **2006**, *71*, 9849−9852.

(24) McClelland, R. A.; Ren, D.; D'Sa, R.; Ahmed, A. R. Acidity Constants and Reactivities of the Benzidine and N,N-Dimethylbenzidine Dications, the Two Electron Oxidation Intermediates of Benzidine Carcinogens. *Can. J. Chem.* **2000**, *78*, 1178−1185.

(25) Kratochvill, B.; Zatko, D. A. Oxidation of Some Arylamines by Copper(II) in Acetonitrile. *Anal. Chem.* **1968**, *40*, 422−424.

(26) Aravindan, P.; Maruthamuthu, P.; Dharmalingam, P. Kinetics of the Formation and Decay of Benzidine Mono Radical Cation in Aqueous Solution. *Bull. Chem. Soc. Jpn.* **1997**, *70*, 37−45.

(27) Desmarets, Chr.; Champagne, B.; Walcarius, A.; Bellouard, Chr.; Omar-Amrani, R.; Ahajji, A.; Fort, Y.; Schneider, R. Facile Synthesis and Characterization of Naphthidines as a New Class of Highly Nonplanar Electron Donors Giving Robust Radical Cations. *J. Org. Chem.* **2006**, *71*, 1351−1361.

(28) Nascimento, G. M.; Padilha, A. C. M.; Constantino, V. R. L.; Temperini, M. L. A. Oxidation of Anilinium Ions Intercalated in Montmorillonite Clay by Electrochemical Route. *Colloids Surf., A* **2008**, *318*, 245−253.
(29) Nascimento, G. M.; Constantino, V. R. L.; Landers, R. M. L.; Temperini, A. Aniline Polymerization into Montmorillonite Clay: A Spectroscopic Investigation of the Intercalated Conducting Polymer. *Macromolecules* **2004**, *37*, 9373−9385.
(30) Guichard, V.; Bourkba, A.; Poizat, O.; Buntinx, G. Vibrational Studies of Reactive Intermediates of Aromatic Amines. 2. Free-Radical Cation and Dication Resonance Raman Spectroscopy of *N,N,N′,N′*-Tetramethylbenzidine and *N,N,N′,N′*-Tetraethylbenzidine. *J. Phys. Chem.* **1989**, *93*, 4429−4435.
(31) Guichard, V.; Poizat, O.; Buntinx, G. Vibrational Studies of Reactive Intermediates of Aromatic Amines. 3. Triplet (T_1) State Time-Resolved Raman Spectroscopy of *N,N,N′,N′*-Tetramethylbenzidine and *N,N,N′,N′*-Tetraethylbenzidine. *J. Phys. Chem.* **1989**, *93*, 4436−4441.
(32) Wheeler, J.; Nelson, R. F. Electrochemical and Spectroscopic Studies of Cation Radicals. II. Anilinium-Type Radical Ion and Benzidine Dication Visible Spectra. *J. Phys. Chem.* **1973**, *77*, 2490−2492.
(33) Soma, Y.; Soma, M. Adsorption of Benzidines and Anilines on Cu- and Fe-Montmorillonites Studied by Resonance Raman Spectroscopy. *Clay Minerals* **1988**, *23*, 1−12.
(34) Azim, S. A. Photo-Degradation and Emission Characteristics of Benzidine in Halomethane Solvents. *Spectrochim. Acta A* **1999**, *56*, 127−132.
(35) Weinberg, N. L.; Weinberg, H. R. Electrochemical Oxidation of Organic Compounds. *Chem. Rev.* **1968**, *68*, 449−523.
(36) Bondarchuk, S. V.; Minaev, B. F.; Fesak, A. Yu. Theoretical Study of the Triplet State Aryl Cations Recombination: A Possible Route to Unusually Stable Doubly Charged Biphenyl Cations. *Int. J. Quantum Chem.* **2013**, *113*, 2580−2588.
(37) Bondarchuk, S. V.; Minaev, B. F. State-Dependent Global and Local Electrophilicity of the Aryl Cations. *J. Phys. Chem. A* **2014**, *118*, 3201−3210.
(38) Bondarchuk, S. V.; Minaev, B. F. Density Functional Study of Ortho-Substituted Phenyl Cations in Polar Medium and in the Gas Phase. *Chem. Phys.* **2011**, *389*, 68−74.
(39) Bondarchuk, S. V.; Minaev, B. F. The Singlet−Triplet Energy Splitting of π-Nucleophiles as a Measure of their Reaction Rate with Electrophilic Partners. *Chem. Phys. Lett.* **2014**, *607*, 75−80.
(40) Bondarchuk, S. V.; Minaev, B. F. About Possibility of the Triplet Mechanism of the Meerwein Reaction. *J. Mol. Struct.: THEOCHEM* **2010**, *952*, 1−7.
(41) Minaev, B. F.; Bondarchuk, S. V.; Girtų, M. DFT Study of Electronic Properties, Structure and Spectra of Aryl Diazonium Cations. *J. Mol. Struct.: THEOCHEM* **2009**, *904*, 14−20.
(42) Minaev, B. F.; Bondarchuk, S. V. Role of Triplet States of Aryldiazonium Cations in the Meerwein Reaction. *Russ. J. Appl. Chem.* **2009**, *82*, 840−845.
(43) Minaev, B. F.; Bondarchuk, S. V.; Fesak, A. Yu. Structure and Spectral Properties of Phenyldiazonium Tetrachlorocuprate(II). *Russ. J. Appl. Chem.* **2010**, *83*, 36−43.
(44) Ogura, T.; Akai, N.; Shibuya, K.; Kawai, A. Charge-Transfer Electronic Absorption Spectra of 1-Ethylpyridinium Cation and Halogen Anion Pairs in Dichloromethane and as Neat Ionic Liquids. *J. Phys. Chem. B* **2013**, *117*, 8547−8554.
(45) Katoh, R.; Hara, M.; Tsuzuki, S. Ion Pair Formation in [bmim]I Ionic Liquids. *J. Phys. Chem. B* **2008**, *112*, 15426−15430.
(46) Kohn, W.; Sham, L. J. Self-Consistent Equations Including Exchange and Correlation Effects. *Phys. Rev. A* **1965**, *140*, A1133−A1138.
(47) Becke, A. D. Density-Functional Thermochemistry. III. The Role of Exact Exchange. *J. Chem. Phys.* **1993**, *98*, 5648−5652.
(48) Lee, C.; Yang, W.; Parr, R. G. Development of the Colle-Salvetti Correlation-Energy Formula into a Functional of the Electron Density. *Phys. Rev. B* **1988**, *37*, 785−789.
(49) Krishnan, R.; Binkley, J. S.; Seeger, R.; Pople, J. A. Self-Consistent Molecular Orbital Methods. XX. A Basis Set for Correlated Wave Functions. *J. Chem. Phys.* **1980**, *72*, 650−654.
(50) Hay, P. J.; Wadt, W. R. Ab Initio Effective Core Potentials for Molecular Calculations − Potentials for the Transition-Metal Atoms Sc to Hg. *J. Chem. Phys.* **1985**, *82*, 270−283.
(51) Miertuš, S.; Scrocco, E.; Tomasi, J. Electrostatic Interaction of a Solute with a Continuum. A Direct Utilizaion of Ab Initio Molecular Potentials for the Prevision of Solvent Effects. *Chem. Phys.* **1981**, *55*, 117−129.
(52) Yanai, T.; Tew, D. P.; Handy, N. C. A New Hybrid Exchange−Correlation Functional using the Coulomb-Attenuating Method (CAM-B3LYP). *Chem. Phys. Lett.* **2004**, *393*, 51−57.
(53) Frisch, M. J.; Trucks, G. W.; Schlegel, H. B.; Scuseria, G. E.; Robb, M. A.; Cheeseman, J. R.; Scalmani, G.; Barone, V.; Mennucci, B.; Petersson, G. A.; et al. *Gaussian 09, Revision A.02*; Gaussian, Inc.: Wallingford, CT, 2009.
(54) Gorelsky, S. I. *SWizard program*; University of Ottawa: Ottawa, Canada, 2013; http://www.sg-chem.net/.
(55) Keith, T. A. *AIMAll, Version 10.07.25*; TK Gristmill Software: Overland Park, KS, 2010. Available at www.aim.tkgristmill.com.
(56) Lu, T.; Chen, F. Multiwfn: A Multifunctional Wavefunction Analyzer. *J. Comput. Chem.* **2012**, *33*, 580−592.
(57) de Proft, F.; Van Alsenoy, C.; Peeters, A.; Langenaeker, W.; Geerlings, P. Atomic Charges, Dipole Moments, and Fukui Functions using the Hirshfeld Partitioning of the Electron Density. *J. Comput. Chem.* **2002**, *23*, 1198−1209.
(58) *Materials Studio 5.5*; Accelrys, Inc.: San Diego, CA, 2008.
(59) Klamt, A.; Schüürmann, G. COSMO: A New Approach to Dielectric Screening in Solvents with Explicit Expressions for the Screening Energy and its Gradient. *J. Chem. Soc., Perkin Trans. 2* **1993**, 799−805.
(60) Becke, A. D.; Edgecombe, K. E. A Simple Measure of Electron Localization in Atomic and Molecular systems. *J. Chem. Phys.* **1990**, *92*, 5397−5403.
(61) Schmider, H. L.; Becke, A. D. Chemical Content of the Kinetic Energy Density. *J. Mol. Struct. (Theochem)* **2000**, *527*, 51−61.
(62) Sjoberg, P.; Murray, J. S.; Brinck, T.; Politzer, P. Average Local Ionization Energies on the Molecular Surfaces of Aromatic Systems as Guides to Chemical Reactivity. *Can. J. Chem.* **1990**, *68*, 1440−1443.
(63) Parr, R. G.; Ayers, P. W.; Nalewajski, R. F. What Is an Atom in a Molecule? *J. Phys. Chem. A* **2005**, *109*, 3957−3959.
(64) Johnson, E. R.; Keinan, S.; Mori-Sánchez, P.; Contreras-García, J.; Cohen, A. J.; Yang, W. Revealing Noncovalent Interactions. *J. Am. Chem. Soc.* **2010**, *132*, 6498−6506.
(65) Bader, R. F. W. *Atoms in molecules. A quantum theory*; Clarendon Press: Oxford, U.K., 1990.
(66) Baryshnikov, G. V.; Minaev, B. F.; Minaeva, V. A.; Baryshnikova, A. T.; Pittelkow, M. DFT and QTAIM Study of the Tetra-*tert*-Butyltetraoxa[8]circulene Regioisomers Structure. *J. Mol. Struct.* **2012**, *1026*, 127−132.
(67) Baryshnikov, G. V.; Minaev, B. F.; Minaeva, V. A.; Nenajdenko, V. G. Single Crystal Architecture and Absorption Spectra of Octathio[8]circulene and *sym*-Tetraselenatetrathio[8]circulene: QTAIM and TD-DFT Approach. *J. Mol. Model.* **2013**, *19*, 4511−4519.
(68) Bushmarinov, I. S.; Lyssenko, K. A.; Antipin, M. Yu. Atomic Energy in the 'Atoms in Molecules' Theory and its Use for Solving Chemical Problems. *Russ. Chem. Rev.* **2009**, *78*, 283−302.
(69) Bauzá, A.; Quiñonero, D.; Deyá, P. M.; Frontera, A. Estimating Ring Strain Energies in Small Carbocycles by Means of the Bader's Theory of 'Atoms-in-Molecules'. *Chem. Phys. Lett.* **2012**, *536*, 165−169.
(70) Ayers, P. W.; Yang, W.; Bartolotti, L. J. Fukui Function. In *Chemical Reactivity Theory: A Density Functional View*;Chattaraj, P. K., Ed.; CRC Press: Boca Raton, FL, 2009; Vol. *18*, pp 255−267.
(71) Morell, Chr.; Grand, A.; Toro-Labbé, A. New Dual Descriptor for Chemical Reactivity. *J. Phys. Chem. A* **2005**, *109*, 205−212.
(72) Bird, C. W. A New Aromaticity Index and its Application to Five-Membered Ring Heterocycle. *Tetrahedron* **1985**, *41*, 1409−1414.

(73) Lu, T.; Chen, F. Bond Order Analysis Based on the Laplacian of Electron Density in Fuzzy Overlap Space. *J. Phys. Chem. A* **2013**, *117*, 3100−3108.
(74) Trotter, J. The Crystal and Molecular Structure of Biphenyl. *Acta Crystallogr.* **1961**, *14*, 1135−1140.
(75) Matta, C. F.; Hernandez-Trujillo, J.; Tang, T.-H.; Bader, R. F. W. Hydrogen − Hydrogen Bonding: A Stabilizing Interaction in Molecules and Crystals. *Chem.—Eur. J.* **2003**, *9*, 1940−1951.
(76) Poater, J.; Solà, M.; Matthias Bickelhaupt, F. Hydrogen−Hydrogen Bonding in Planar Biphenyl, Predicted by Atoms-In-Molecules Theory, Does Not Exist. *Chem.—Eur. J.* **2006**, *12*, 2889−2895.
(77) O'Hagan, D. Understanding Organofluorine Chemistry. An Introduction to the C−F Bond. *Chem. Soc. Rev.* **2008**, *37*, 308−319.
(78) Minaev, B. F.; Baryshnikov, G. V.; Slepets, A. A. Structure and Spectral Properties of Triphenylamine Dye Functionalized with 3,4-Propylenedioxythiophene. *Opt. Spectrosc.* **2012**, *112*, 829−835.
(79) Baryshnikov, G. V.; Minaev, B. F.; Minaeva, V. A.; Podgornaya, A. T.; Ågren, H. Application of Bader's Atoms in Molecules Theory to the Description of Coordination Bonds in the Complex Compounds of Ca^{2+} and Mg^{2+} with Methylidene Rhodanine and Its Anion. *Russ. J. Gen. Chem.* **2012**, *82*, 1254−1262.
(80) Creason, S. C.; Wheeler, J.; Nelson, R. F. Electrochemical and Spectroscopic Studies of Cation Radicals. I. Coupling Rates of 4-Substituted Triphenylaminium Ion. *J. Org. Chem.* **1972**, *37*, 4440−4446.
(81) Itoh, T. Fluorescence and Phosphorescence from Higher Excited States of Organic Molecules. *Chem. Rev.* **2012**, *112*, 4541−4568.